

SUBARU/HDS STUDY OF HE 1015–2050: SPECTRAL EVIDENCE OF R CORONAE BOREALIS LIGHT DECLINE

Aruna Goswami¹ and Wako Aoki²

¹*Indian Institute of Astrophysics, Bangalore 560034, India; aruna@iiap.res.in*

²*National Astronomical Observatory, Mitaka, Tokyo 181-8588, Japan*

ABSTRACT

Hydrogen deficiency and a sudden optical light decline by about 6-8 mag are two principal characteristics of R Coronae Borealis (RCB) stars. The high latitude carbon star HE 1015–2050 was identified as a hydrogen-deficient carbon star from low-resolution spectroscopy. Photometric data of the Catalina Real-Time Transient Survey gathered between 2006 February and 2012 May indicate that the object exhibits no variability. However, a high-resolution ($R \sim 50,000$) optical spectrum of this object obtained with the 8.2m Subaru telescope using High Dispersion Spectrograph on the 2012 January 13 offers sufficient spectral evidences for the object being a cool HdC star of RCB type undergoing light decline. In contrast to the Na I D broad absorption features, seen in the low-resolution spectra on several occasions, the high-resolution spectrum exhibits Na I D₂ and D₁ features in emission. A few emission lines due to Mg I, Sc II, Ti I, Ti II, Fe II and Ba I are also observed in the spectrum of this object for the first time. Such emission features combined with neutral and singly ionized lines of Ca, Ti, Fe, etc., in absorption are reportedly seen in RCBs spectra in the early stage of decline or during the recovery to maximum. Further, the light decline of RCBs is ascribed to the formation of a cloud of soot that obscures the visible photosphere. Presence of such circumstellar material is evident from the polarimetric observations with an estimated V-band percentage polarization of $\sim 1.7\%$ for this object.

Subject headings: stars: carbon - stars: chemically peculiar - stars: individual (HE 1015–2050) - stars: late-type - stars: low-mass

1. INTRODUCTION

Hydrogen-deficient carbon (HdC) stars and R Coronae Borealis (RCB) type stars form a rare class of carbon-rich supergiants (Clayton (1996), Clayton (2012) for a general review). The deep minima and infrared excesses that are characteristics of RCB stars are absent in HdC stars (Warner (1967); Feast & Glass (1973); Feast et al. (1997)). These stars have spectra similar to F-G supergiants, but show only weak absorption features of hydrogen while molecular bands of carbon are strong (in cool RCBs and HdCs). The most promising scenario for the origin of these objects is that they are post-asymptotic giant branch (post-AGB) stars, which are low- to intermediate-mass stars at the evolutionary state from AGB to white dwarfs, particularly objects which experience a final helium flash (Iben et al. (1996)). However, many other scenarios, including a merger of two white dwarfs, have also been proposed (Webbink (1984); Renzini (1990); Staff et al. (2012)).

Chemical composition studies of RCB stars suggest the presence of material in their atmosphere is being exposed to s-processing. Asplund et al. (2000) find that all RCB stars show some enhancement of s-process elements relative to Fe ($[Y/Fe] = 0.8$; $[Ba/Fe] = 0.4$). Extraordinary overabundances of Y and Ba in U Aqr are also reported by Vanture et al. (1999) with estimates of $[Y, Zr/Fe] \geq +3.0$ and $[Ba/Fe] = 2.1$. Light neutron-capture elements like Sr, Y, and Zr are usually attributed to the weak component of the s-process, which is the neutron-capture process with relatively long time scale and small neutron exposure (Käppeler et al. (2011)). Massive stars in He- or C-burning phase are suggested as the astrophysical site of the weak s-process, but there is no direct observational evidence to support this scenario.

From low-resolution spectroscopic analysis of a large number of faint high latitude carbon stars of Hamburg/ESO survey, Goswami et al. (2010) have identified HE 1015–2050 to be an HdC star. The object has an IR excess, the observed magnitudes detected by NASA’s *Wide-field Infrared Survey Explorer* (WISE) are 14.663 at 3.4 and 4.6 μm bands, 12.887 at 12 μm and 9.195 at 22 μm band. The object is also monitored by the Catalina Real-Time Transient Survey (CRTS); light-curve data obtained between 2006 February and 2012 May indicate that the object exhibits no variability at the level of measurement uncertainties (Andrew Drake, private communication 2012). In this Letter, we discuss its high-resolution spectrum and confirm its hydrogen deficiency. Further, we find that the spectrum displays features that are reminiscent of RCBs at early decline or near recovery to maximum. The spectrum is characterized by strong features of Sr and Y. There are no obvious stronger features of heavier elements (i.e., Mo, Ba) indicating that this object can be a source of weak s-process.

2. OBSERVATIONS AND DATA REDUCTION

The high-resolution spectroscopic observations of HE 1015–2050 was carried out with the High Dispersion Spectrograph (HDS) of the 8.2m Subaru Telescope (Noguchi et al. (2002)) on 2012 January 13. The spectrum was taken with a 30 minute exposure at a resolving power of $R \sim 50,000$. The observed bandpass ran from about 4010 Å to 6800 Å with a gap of about 75 Å from 5355 Å to 5430 Å due to the physical spacing of the CCD detectors. The low-resolution ($R \sim 1300$) spectrum obtained with 2m HCT at IAO, Hanle is taken from (Goswami et al. (2010)). The data were reduced, in the standard fashion, using IRAF¹ spectroscopic data reduction package.

3. RADIAL VELOCITY

A selection of about 30 absorption lines are used to determine the radial velocity of the object HE 1015–2050. Velocities are derived from the central cores of lines. Mean Heliocentric radial velocity is estimated to be $\sim 18 \pm 1.5 \text{ km s}^{-1}$. Radial velocity survey of RCB stars by Lawson & Kilkenny (1996) records a typical peak-to-peak variations of 10–20 km s^{-1} . The velocities estimated from the emission features of H_α , Na I D_2 and D_1 , Sc II $\lambda 5684.19$ are, respectively, 17.1, 19.3, 19.6, and 21.8 km s^{-1} , and are similar to the velocity derived from the photospheric absorption lines. There is, however, evidence that the narrow emission lines are blueshifted relative to the pre-decline absorption lines (e.g. R CrB, Cottrell et al. (1990)).

4. SPECTRAL CHARACTERISTICS

During deep declines of RCBs (e.g., R CrB and RY Sgr) the forming dust cloud extinguishes the photospheric light and a rich narrow-line emission spectrum appears consisting of neutral and singly ionized metals (Payne-Gaposchkin (1963); Alexander et al (1972); Clayton (1996)). Most of these lines referred as E1 (Alexander et al (1972)) are short-lived that fade within two or three weeks and are replaced by a broad-line spectrum. Some of the early-decline narrow emission lines remain strong for an extended period of time. These lines referred as E2 are mostly low excitation lines, and primarily multiples of Sc II and Ti II. The Sc II $\lambda 4246$ line is one of the strongest lines in the E2 spectrum of RCB stars in decline

¹IRAF is distributed by the National Optical Astronomical Observatory, which is operated by the Association for Universities for Research in Astronomy, Inc., under contract to the National Science Foundation.

(Rao et al. (1999)). The spectrum of HE 1015–2050 shows narrow-line emission features as well as broad absorption features, leading us to believe that the spectrum was acquired when the object was obscured by forming dust. We put forward our arguments supporting this idea in the following sections.

4.1. Spectral Characteristics: Hydrogen Deficiency

In Figure 1, we show a comparison of the spectrum of HE 1015–2050 with the spectrum of HD 26, a hydrogen normal CH star, in the wavelength region 4310–4330 Å. The features due to G band of CH, seen in deep absorption in HD 26, are distinctly shallow in HE 1015–2050. We have also compared the H_α feature in HE 1015–2050 with its counterpart in HD 26 (Figure 1, right panel). While H_α appears as a strong absorption feature in the spectrum of HD 26, in the spectrum of HE 1015–2050 we note an emission feature at the absorption core. The velocity estimated from the H_α emission feature is $\sim +17.1 \pm 1.5$ km s⁻¹, very similar to the velocity derived from the photospheric absorption lines.

Marginal detection or non-detectability of H_β and H_γ features could also be an evidence for hydrogen deficiency. Weak and shallow features of H_β (Figure 5) and H_γ in the spectrum of HE 1015–2050 are seen with marginally detected emissions at the absorption cores. The Balmer lines, which are typically very weak in RCB stars, are seen going into emission in a few cases (i.e., V 854 Cen, Rao & Lambert (1993); Clayton et al. (1993)). Strong Balmer lines and features of CH bands are seen in the spectrum of V 854 Cen (Kilkenny & Marang (1989); Lawson & Cottrell (1989)).

4.2. Spectral Characteristics: Carbon Molecular Bands

The spectrum of HE 1015–2050 contains lines of neutral atomic carbon, and lines of blue-degraded Swan system of C₂ bands. The red isotopic bands involving ¹³C are not normally present in RCB stars (Lloyd Evans et al. 1991). As expected, the (1,0) ¹³C¹²C λ4744 band is much weaker than the (1,0) ¹²C¹²C λ4737 band. Among the C₂ molecular bands, ¹²C¹²C λ6122, and ¹²C¹²C λ5635 are weak but distinctly seen in absorption with redshifted bandheads. Bands of ¹²C¹³C λ6100 and ¹²C¹³C λ6168 are not detected.

As in the case of normal RCBs the CN bands of (4,0) λ6206, (6,1) λ5730, and (7,1) λ5239 are weak or absent in the spectrum of HE 1015–2050. Strong blue-degraded CN band, (0,1) λ4216 is however seen in RCBs. In the spectrum of HE 1015–2050, the strong SrII feature that appears at the location of 4215.2 Å is likely to have been affected by contributions

from this band. Many C I absorption lines are reportedly observed in RCBs in decline (e.g., RY Sgr) which fill in but never go into emission (Alexander et al. 1972). In some declines, the Swan bands of C₂ are seen in emission (Payne-Gaposchkin (1963); Whitney et al. (1992); Rao & Lambert (1993)).

4.3. Spectral Characteristics: Emission Features

Na I D₂ and D₁ features. In Figure 2, we show the Na I D features of HE 1015–2050. In the low resolution ($\lambda/\delta\lambda \sim 1300$) spectrum, Na I D₂ and D₁ features are not resolved and appear in absorption (Figure 2, lower panel). These features are clearly resolved in the high resolution ($\lambda/\delta\lambda \sim 50,000$) spectrum and appear in emission (Figure 2, upper panel). Emission features of Na I D₁ and D₂ are reportedly seen in decline spectra of RCBs; at maximum these features appear in absorption. The appearance of Na I D₂ and D₁ in emission in the high-resolution spectrum of HE 1015–2050 is a clear indication that the spectrum is acquired at its early decline or near recovery to maximum. In the R CrB decline spectra, these two features in emission show a large variation throughout the decline (Rao et al. 1999).

Forbidden oxygen lines. Sharp emission features of the forbidden lines of [OI] 5577, 6300 and 6363 Å are identified in the spectrum of HE 1015–2050. The estimated flux ratio ($[F(6300) + F(6363)]/F(5577)$) is ~ 0.29 . Rao et al. (1999), have reported a value of ~ 18 for this flux ratio throughout the 1995-1996 decline of R CrB.

Atomic lines: emission features of Sc, Mg, Ti, Fe, Ba. We have made a weak detection of the line Sc II $\lambda 4246.8$ in emission in the spectrum of HE 1015–2050. This line is one of the strongest lines in the "E2" spectrum of RCB stars in decline (e.g., Rao et al. (1999)). Sc II line at 5657.88 Å also appears in emission. As shown in Figure 3, an emission feature at the absorption core of Mg I at 5167.3 Å is seen in its spectrum. A few other emission features such as, Mg I 5183.6 Å, Ti I 5173.7 Å, Ti II 5185.9 Å and Fe II 5197.5 Å are also noticed in the spectrum (Figure 3). As shown in Figure 4, lines of Sc II $\lambda 5684.2$ and Ba I $\lambda 6498.7$ are clearly seen in emission. Emission lines of Sc II $\lambda 5684$, Fe II $\lambda 6247$, Ba II $\lambda 6497$, Fe II $\lambda 5362$, Fe I $\lambda\lambda 5405, 5371, 5447$, Ti II $\lambda\lambda 5490, 5492$, Si I $\lambda 4102$, Zr II $\lambda 4096$ are reportedly seen in the 1995 October 18 decline spectrum of R CrB with red absorption components (Rao et al. 1999). Some unidentified emission features are known to exist in RCB decline spectra (Whitney et al. (1992); Asplund (1995)); the spectrum of HE 1015–2050 also displays a number of emission features that remain unidentified.

4.4. Spectral Characteristics: Absorption Spectrum

Helium. Among the four lines from the triplet series of neutral helium seen in R CrB’s decline spectrum (Rao et al. 1999), except for 5876 Å the other three 3889 Å, 7065 Å, and 10830 Å are out of the wavelength region considered here. However, He I lines of D3 5876 Å are not detected either in emission or absorption in the spectrum of HE 1015–2050. This line is observed in broad emission in R CrB’s decline spectrum (Rao et al. (1999)). It is possible that this line has also been filled-in by emission but has not risen above the continuum. Other He I triplets at 4471 Å and 4713 Å and singlet lines of He I at 4922 Å and 5015 Å are not detected in the spectrum of HE 1015–2050.

Lithium. Features due to Li are not detected in the spectrum of this object. Only four RCB stars (e.g., UW Cen, R CrB, RZ Nor, and SU Tau) are known to be Li-rich with Li abundance ranging from 2.6 to 3.5 (Asplund et al. (2000)). Pollard et al. (1994) reported the presence of Li in two of the LMC R CrB stars. Vanture et al. (1999) mention a tentative identification of the Li I 6708 Å line in U Aqr. Z UMi, a cool RCB star also shows lithium (Kipper & Klochkova (2006)). In Figure 5, the location of Li I at 6708 Å in the spectrum of HE 1015–2050 is shown, compared with its counterpart in Z Umi, where this feature is seen strongly. The spectrum of Z Umi is taken from Goswami et al. (1997).

Atomic lines: Na, Mg, Si, Ca, Ti, V, Cr, Mn, Fe, Co, Ni. Many neutral and singly ionized lines of these elements are detected in the spectrum of HE 1015–2050. Some of these lines show filled-in emission. For instance, Ca I line at 4226.7 Å and Fe I line at 4222.2 Å detected in absorption show filled-in emission at the absorption cores, whereas NaI line at 5688.2 Å and Ca I line at 4094.9 Å also detected in absorption do not show any filled-in emission. Several neutral and singly ionized lines of FeI are also detected. Lines due to V, Cr, Mn, Co, and Ni are also seen in the spectrum in blends with contributions from other atomic lines. Cr I line at 5674.1 Å is clearly detected in absorption. A few absorption features due to Fe I and Ti I are shown in Figure 4 along with a Mg I absorption feature at 5172.7 Å.

Atomic lines: Sr, Y, Mo, Ba, Ce. The spectrum of HE 1015–2050 is found to exhibit strong features of Strontium. Sr II λ 4077.7 is detected as a strong absorption feature that seems to show filled-in emission. Sr II line at 4215.5 Å is also detected as a strong feature in absorption. This feature is likely to have been affected by contributions due to strong blue-degraded (0,1) CN 4216 band. These two Sr features are shown in Figure 5. Although detected clearly, Ba II at 4554 Å (Figure 5) and 6496 Å (Figure 4) are obviously not stronger than Sr lines. While Ba II line at 4554.036 Å is observed with an equivalent width of 131m Å we have made a marginal detection of Ba II feature at 6496.9 Å in absorption. Lines due to Y II and Ce II are also detected in the spectrum in blends with contribution from other

atomic lines. We have made a weak detection of the Mo I line at 5689.2 Å in absorption (Figure 5).

4.5. Circumstellar Environment: Polarimetric Evidence

The photometric light variability of RCBs has been ascribed to formation of a cloud soot that obscures the visible photosphere (Loreta (1934); O’Keefe (1939)). Presence of circumstellar material is supported by our polarimetric observations of 2012 April 21. The estimated V-band percentage polarization for this object is quite significant with a value of $\sim 1.7\%$ (Goswami & Karinkuzhi (2013), A. Goswami et al., in preparation for details). The interstellar polarization is presumed to be negligible because of the object’s high Galactic latitude. Information on polarization estimates measured in RCB declines are limited to only a few objects (Serkowski & Kruszewski (1969); Stanford et al. (1988); Whitney et al. (1992)). Coyne & Shawl (1973) found large polarization variations associated with a brightness minimum of R CrB in 1972; during a decline of 7 mag, the polarization in B band was found to vary from 0.29% to 3.29% over three weeks. A number of studies have confirmed that the dust causing the declines is carbon rich (Holm et al. (1982); [Hecht et al. (1984); Wright et al. (1989); Hecht (1991)).

5. CONCLUDING REMARKS

The high-resolution spectrum of the HdC star HE 1015–2050, acquired on 2012 January 13, shows features that are reminiscent of RCBs at early decline or near recovery to maximum. Optical light decline in RCBs is attributed to the formation of clouds of carbon dust (O’Keefe 1939). Presence of circumstellar material is supported by our polarimetric observation.

Appearance of a narrow-line emission spectrum consisting of lines of neutral and singly ionized metals, and a few broad lines including Ca II H and K, the Na I D lines is a common characteristics of RCBs in decline (Payne-Gaposchkin (1963); Alexander et al (1972); Clayton (1996); Rao et al. (1999)). With emission lines of Na I D₁ and Na I D₂, Sc II, Mg I etc. the spectrum of HE 1015–2050 seems to show characteristics of an RCB decline spectrum.

The non-detection of Li features may be used as a clue for the production mechanism of this object. Among the two most promising scenarios for the origin of RCBs Li enhancements are consistent with the FF models as in the case of Sakurai’s object (Lambert (1986),

Asplund et al. (1998)). However, a high carbon isotopic ratios as well as enhancement of ^{18}O with no Li production are expected from WD merger scenario. From these, the latter is a more likely production scenario for this object; however, knowledge of the carbon and oxygen isotopic ratios would be necessary to support this.

The spectrum shows strong features of Sr but no obvious strong features of heavier elements (i.e., Mo, Ba). It has been suggested that the rapid proton-capture (rp) process that occurs during the merger of a white dwarf and a neutron star is expected to produce a large excess of Mo ($Z = 42$) compared to Sr and Y, with no excess of barium and other heavy elements (Cannon (1993)). It is therefore unlikely that the rp-process is responsible for the surface composition of this object. As Thorne-Zytkow objects are suggested to reveal the products of rp-process in their surface composition, HE 1015–2050 does not form a good candidate for a Thorne-Zytkow object.

Strong spectral features of Sr and weak detection of Mo and Ba indicate that its atmosphere is enriched with material resulting from weak s-process. Several possibilities exist for giving rise to such atmospheres. The object may have been formed out of material which is already enriched with s-process material. Alternatively, the object may have been in a binary system with a companion that had undergone unusual s-process enrichment and had transferred mass to this object. However, the binary status of the object cannot be confirmed at present, and also, except for DY Cen (Rao et al. (2012)) none of the RCB and HdC stars is known to be binary (Clayton (1996)). Another possibility concerns the fact that the spectrum does not show enhancement in heavy s-process elements, and hence, it seems necessary for the s-process to produce only light s-process material. This requires a low neutron density. It was shown by Smith (2005) that assuming all other parameters same, higher neutron densities produce larger amounts of heavier elements than of lighter ones. As suggested for U Aqr (Bond & Luck (1979)) HE 1015–2050 could also be an He-C core of an evolved star of near-solar initial mass that ejected its H-rich envelope at the He core flash. A single neutron exposure occurred at the flash, resulting in a brief neutron irradiation producing more of the s-process elements. Detailed chemical composition studies based on high-resolution spectra taken at maximum would be worthwhile to unearth the production mechanism.

Acknowledgment

We thank the referee Geoff Clayton for his many useful suggestions. This work made use of the SIMBAD astronomical database, operated at CDS, Strasbourg, France, and the NASA ADS, USA.

REFERENCES

- Alexander, J. B., Andrews, P. J., Catchpole, R. M., et al. 1972, *MNRAS*, 158, 305
- Asplund, M. 1995, *A&A*, 294, 763
- Asplund, M., Gustafsson, B., Lambert, D. L., et al. 2000, *A&A*, 353, 287
- Asplund, M., Rao, N. K., Lambert, D. L., et al. 1998, *A&A*, 332, 651
- Bond, H.E., Luck, R.E., & Newman, M. J. 1979, *ApJ*, 233, 205
- Cannon, R. C. 1993, *MNRAS*, 263, 817
- Clayton, G. C. 1996, *PASP*, 108, 225
- Clayton, G. C. 2012, *AAVSO*, 40, 539
- Clayton, G. C., Lawson, W. A., Whitney, B. A., et al. 1993, *MNRAS*, 264, L13
- Cottrell, P. L., Lawson, W. A., & Buchhorn, M. 1990, *MNRAS*, 244, 149
- Coyne, G. V. & Shawl, S. J. 1973, *ApJ*, 186, 961
- Feast, M. W., Carter, B. S., Roberts, G., et al. 1997, *MNRAS*, 285, 317
- Feast, M. W., & Glass, I. S. 1973, *MNRAS*, 161, 293
- Goswami, A. & Karinkuzhi, D. 2013, *A&A*, 549, A68
- Goswami, A., Karinkuzhi, D., & Shantikumar, N. S. 2010, *ApJL*, 723, 238
- Goswami, A., Rao, N. K., & Lambert, D. L. 1997, *PASP*, 109, 796
- Hecht, J. H. 1991, *ApJ*, 367, 635
- Hecht, J. H., Holm, A. V., Donn, B., et al. 1984, *ApJ*, 280, 228
- Holm, A. V., Wu, C. C., & Doherty, L. R. 1982, *PASP*, 94, 548
- Iben, I., Jr., Tutukov, A. V., & Yungelson, L. R. 1996, *ApJ*, 456, 750
- Käppeler, F., Gallino, R., Bisterzo, S., et al. 2011, *RvMP*, 83, 157
- Kilkenny, D. & Marang, F. 1989, *MNRAS*, 238, 1p
- Kipper, T. & Klochkova, V. G. 2006, *BaltA*, 15, 531

- Lambert, D. L. 1986, in IAU Colloq. 87: Hydrogen-deficient Stars and Related Objects, ed. K. Hunger, D. Schönberner, & N. K. Rao (Astrophysics and Space Science Library, Vol. 128; Dordrecht: Reidel), 127
- Lawson, W. A., & Cottrell, P. L. 1989, MNRAS, 240, 689
- Lawson, W. A., & Kilkenny, D. 1996, in ASP Conf. Ser. 96, Hydrogen Deficient Stars, ed. C. S. Jeffery & U. Heber (San Francisco, CA: ASP), 349
- Lloyd Evans, T., Kilkenny, D., & van Wyk, F. 1991, Obs, 111, 244
- Loreta, E. 1934, AN, 254, 151
- Noguchi, K., Aoki, W., Kawanomoto, S., et al. 2002, PASJ, 54, 855
- O’Keefe, J. A. 1939, ApJ, 90, 294
- Payne-Gaposchkin, C. 1963, ApJ, 138, 320
- Pollard, K. R., Cottrell, P. L., & Lawson, W. A. 1994, MNRAS, 268, 544
- Rao, N. K. & Lambert, D. L. 1993, AJ, 105, 1915
- Rao, N. K., Lambert, D. L., Adams, M. T., et al. 1999, MNRAS, 310, 717
- Rao, N. K., Lambert, D. L., Hernandez, G., et al. 2012, ApJL, 760, 3
- Renzini, A. 1990, in ASP Conf. Ser. 11, Confrontation between Stellar Pulsation and Evolution, ed. Carla Cacciari & Gisella Clementini (San Francisco, CA: ASP), 549
- Serkowski, K., & Kruszewski, A. 1969, ApJL, 155, 15
- Smith, V. V. 2005, in ASP Conf. Ser. 336, Cosmic Abundances as Records of Stellar Evolution and Nucleosynthesis in Honor of David L. Lambert, ed. T. G. Barnes, III & F. N. Bash (San Francisco, CA: ASP), 165
- Staff, J. E., Menon, A., Herwig, F., et al. 2012, ApJ, 757, 76
- Stanford, S. A., Clayton, G. C., Meade, M. R., et al. 1988, ApJL, 325, 9
- Vanture, A. D., Zucker, D., & Wallerstein, G. 1999, ApJ, 514, 932
- Warner, B. 1967, MNRAS, 137, 119
- Webbink, R. F. 1984, ApJ, 277, 355

Whitney, B. A., Clayton, G. C., Schulte-Ladbeck, R., et al. 1992, AJ, 103, 1652

Wright, E. L. 1989, ApJL, 346, 89

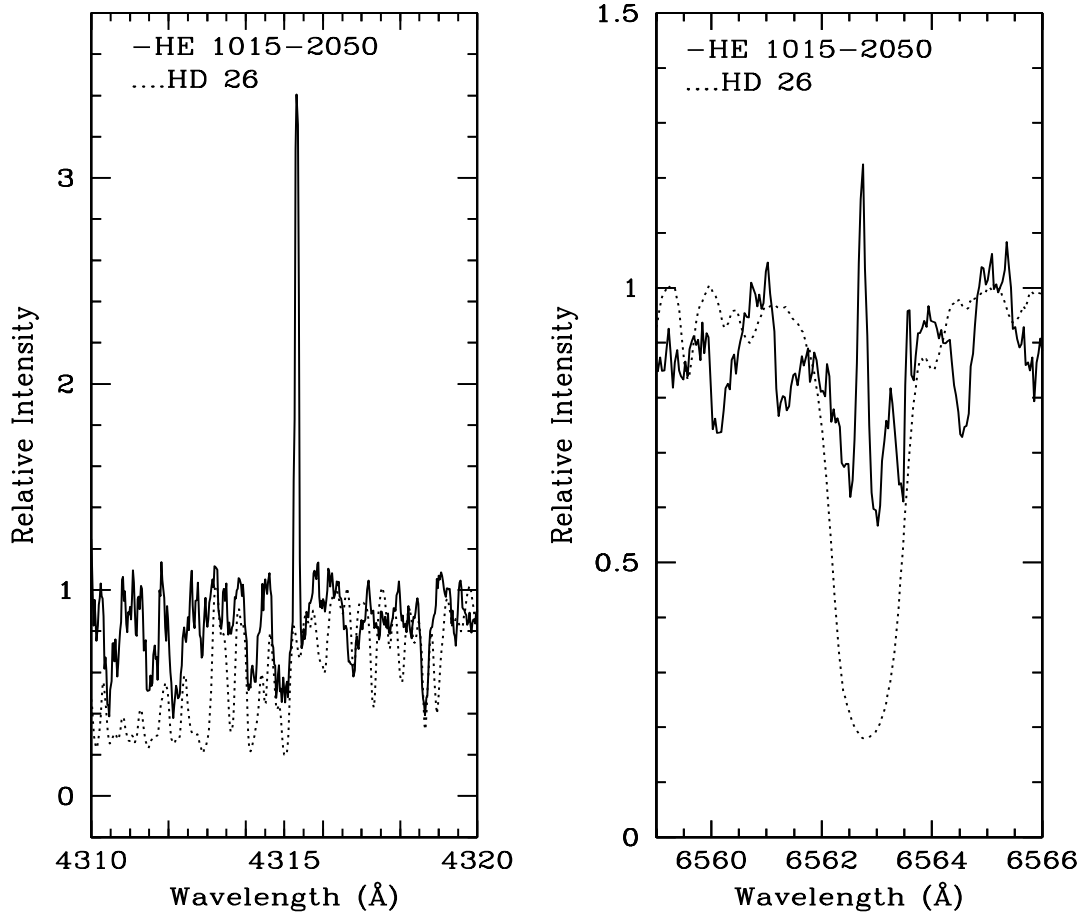


Fig. 1.— Left panel: a comparison between the spectra of HE 1015–2050 and HD 26, a well-known CH star in the wavelength region 4310–4320 Å. Lines due to the G band of CH around 4315 Å are seen in deep absorption in HD 26 and are much weaker in HE 1015–2050. Right panel: while H_{α} appears as a strong absorption feature in HD 26, an emission feature at the absorption core is noticed in the spectrum of HE 1015–2050.

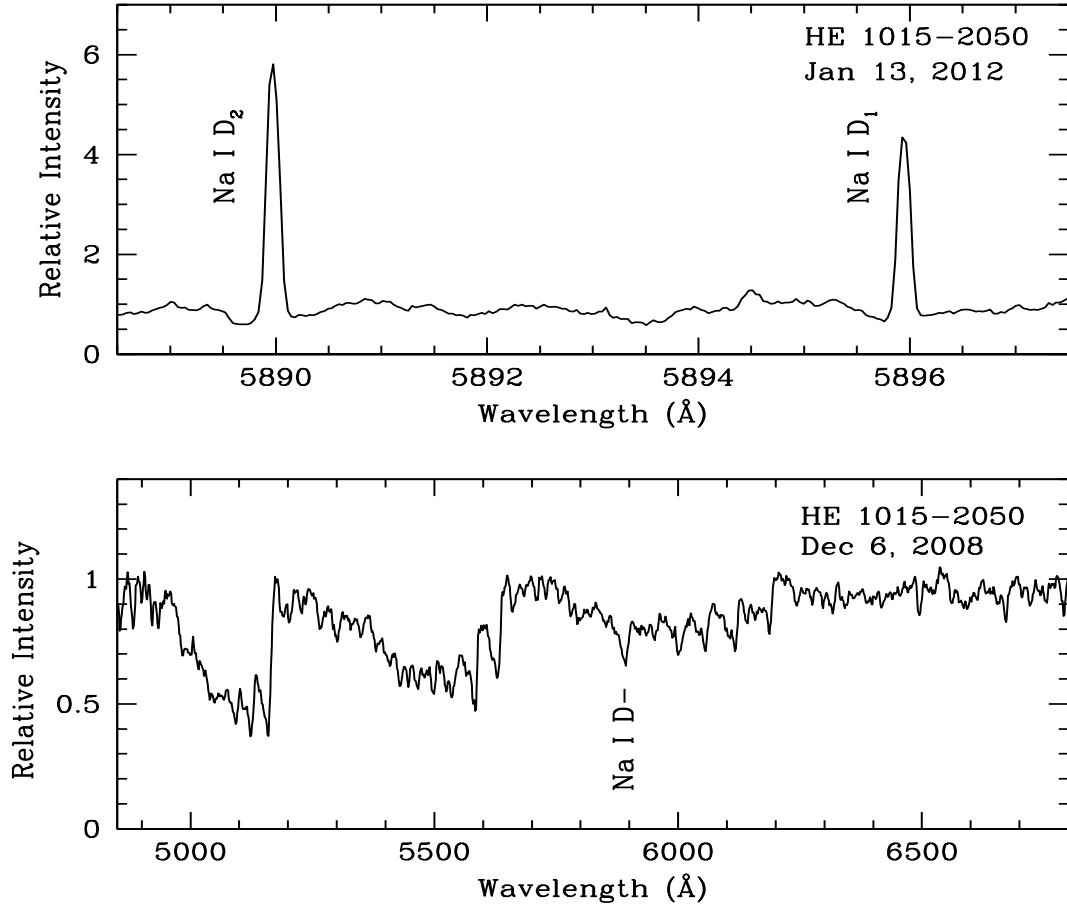


Fig. 2.— Na I D₂ and Na I D₁ that appear as one broad absorption feature in the low-resolution ($R \sim 1300$) spectrum (lower panel) appear in emissions in the high-resolution ($R \sim 50,000$) spectrum (upper panel).

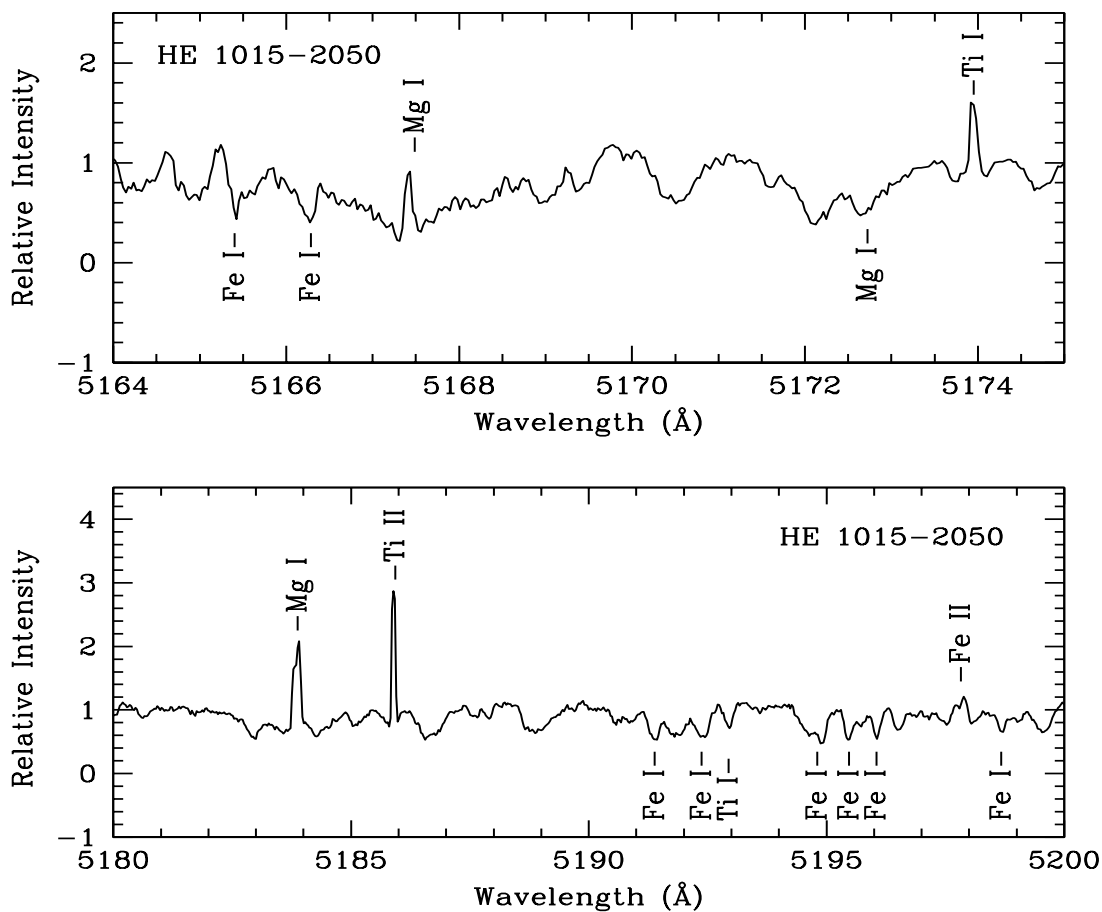


Fig. 3.— Top: the wavelength region 5164-5175 Å of the spectrum is shown. An emission feature at the absorption core of Mg I at 5167.3 Å and Ti I at 5173.7 Å in emission are indicated in the figure. Two absorption features of Fe I and the Mg I line at 5172.7 Å are marked. Bottom: the wavelength region 5180-5200 Å is shown. Emission features of Mg I 5183.6 Å, Ti II 5185.9 Å, and Fe II 5197.5 Å are indicated. Several broad Fe I features and a Ti I feature seen in absorption are marked with vertical lines.

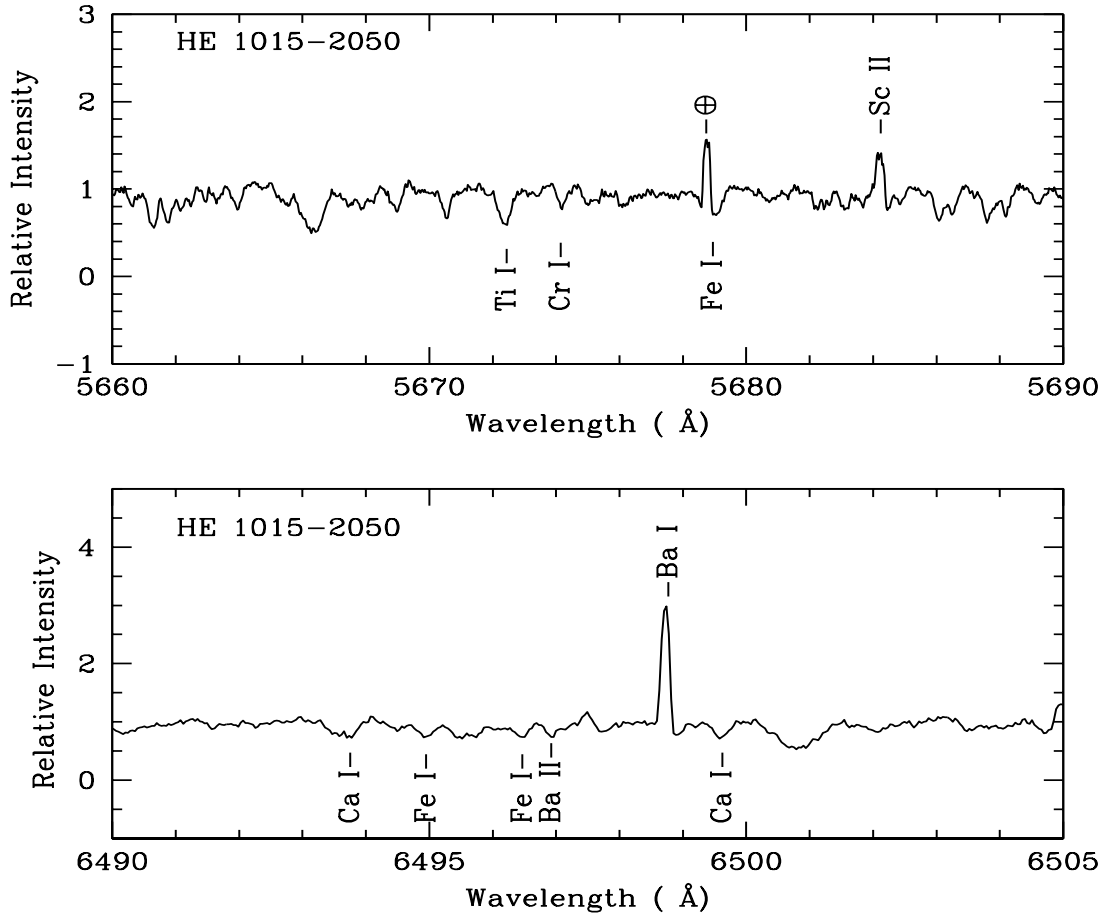


Fig. 4.— Top: the wavelength region 5660-5690 Å of the spectrum is shown. The emission feature of Sc II λ 5684.1 and a few absorption features are indicated. Bottom: the wavelength region 6490-6505 Å of the spectrum is shown. While Ba I λ 6498.7 is detected in emission, Ba II λ 6496.9 is seen weakly in absorption. Absorption features of Ca I and Fe I are also indicated.

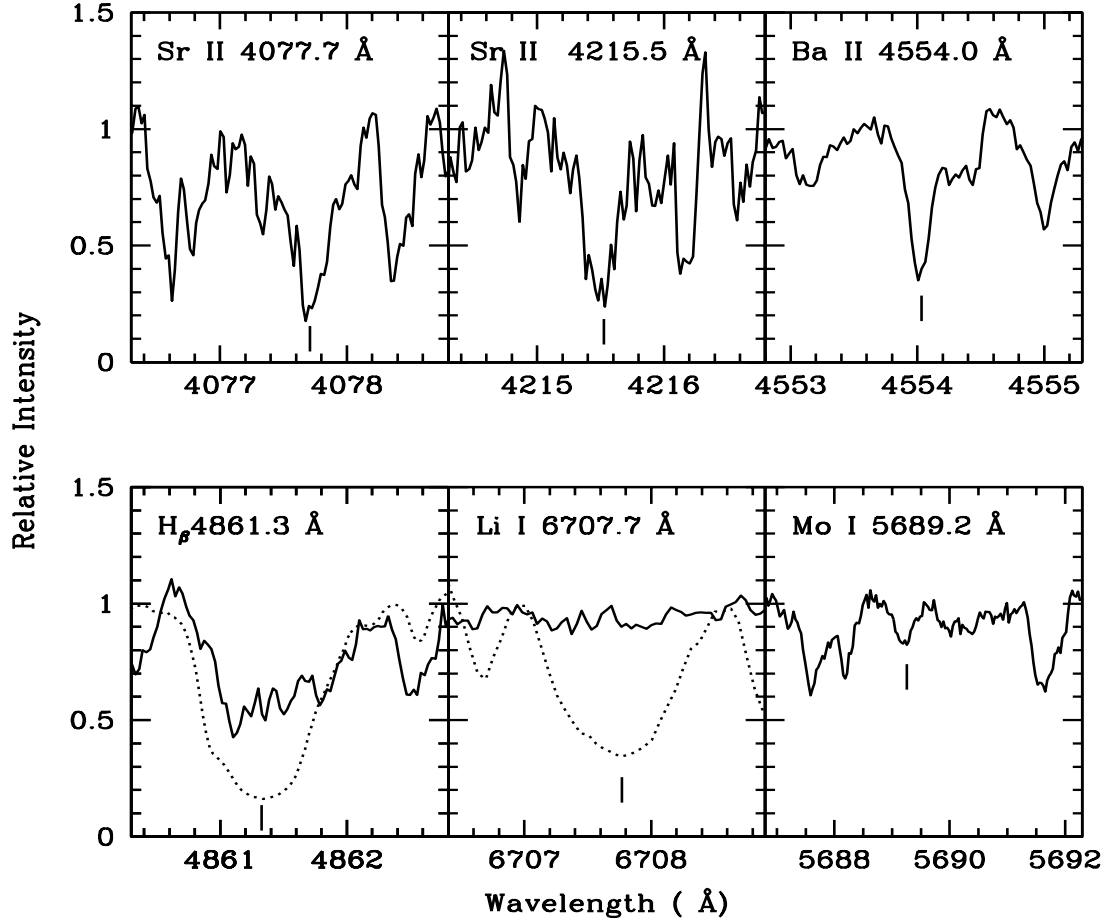


Fig. 5.— Features due to H β , Li, Mo, Sr, and Ba are illustrated. The vertical lines indicate the line centers. The solid lines correspond to HE 1015–2050 in all the panels. In the panel showing H β the dotted lines that correspond to HD 26 and in the panel of Li the dotted lines that correspond to Z Umi, a cool RCB star, are shown for a comparison.